ELSEVIER

Earth and Planetary Science Letters 192 (2001) 159–174

EPSL

www.elsevier.com/locate/epsl

Motion of Africa and Adria since the Permian: paleomagnetic and paleoclimatic constraints from northern Libya

Giovanni Muttoni [a,*], Eduardo Garzanti [b,c], Laura Alfonsi [d], Simonetta Cirilli [e], Daniela Germani [f], William Lowrie [a]

[a] *Institute of Geophysics, ETH Hönggerberg, 8093 Zürich, Switzerland*
[b] *Dipartimento di Scienze Geologiche e Geotecnologie, Università di Milano-Bicocca, Piazza della Scienza, 20126 Milan, Italy*
[c] *CNR-CSGAQ, via Mangiagalli 34, 20133 Milan, Italy*
[d] *Istituto Nazionale di Geofisica e Vulcanologia, Via di Vigna Murata 605, 00143 Rome, Italy*
[e] *Dipartimento di Scienze Geologiche, Università di Perugia, Piazza Università, Perugia, Italy*
[f] *Dipartimento di Scienze della Terra, Università di Milano, via Mangiagalli 34, 20133 Milan, Italy*

Received 5 April 2001; received in revised form 9 July 2001; accepted 10 July 2001

Abstract

Paleomagnetic and biostratigraphic data from the Al Azizia Formation of northwestern Libya, consisting of uppermost Middle Triassic/lowermost Upper Triassic limestones, shed new light on the latitudinal drift of Africa and Adria and related climatic changes. A characteristic component of magnetization carried by magnetite delineates paleomagnetic poles which are coincident with coeval poles from the Southern Alps. Data from this study and the literature are integrated, showing that relatively unrotated remnants of the Adria margin like the Southern Alps (e.g., the Dolomites), Istria, Gargano, Apulia and Iblei moved in close conjunction with Africa since at least Permian times. A Permian–Cenozoic apparent polar wander (APW) curve for Africa/Adria is constructed. The paleolatitude trend for northern Libya calculated from this APW superposed to the zonal latitudinal bands of relative aridity and humidity typical of modern-day climate predicts that northern Libya drifted northwards from the equatorial belt to the arid tropic during the Triassic, and crossed the humid subequatorial/arid subtropical boundary zone at Late Triassic times. This inference is fully supported by Permo-Triassic palynological and facies analysis from this study and the literature. We conclude that a zonal climate model coupled with paleomagnetically constrained paleogeographic reconstructions provides a powerful null hypothesis for understanding past climatic conditions.

Keywords: Libya; Triassic; paleomagnetism; palynology; Africa; Adriatic Plate

1. Introduction

The African affinity of relatively unrotated remnants of the Adria margin (i.e., portions of the Southern Alps, Istria, Gargano, Apulia and Iblei;

* Corresponding author. Present address: Dipartimento di Scienze della Terra, Università di Milano, via Mangiagalli 34, 20133 Milan, Italy. Tel.: +39-2-236-98-203; Fax: +39-2-706-38-261.
E-mail address: giovanni.muttoni1@unimi.it (G. Muttoni).

0012-821X/01/$ – see front matter
PII: S0012-821X(01)00439-3

Fig. 1) has been documented paleomagnetically in a number of papers (e.g., [1–4]). The agreement of Africa and Adria data has been established within typical paleomagnetic resolution of a few degrees for the Early Permian, Late Jurassic to Early Cretaceous and Late Cretaceous. The coherent motion of Africa/Adria has a wide range of geologic implications, from the study of the kinematics of the Alpine arc in the Cenozoic (e.g., [5]) to Tethyan paleogeography at Pangea times (e.g., [6]). Paleomagnetic data from Adria have also been used as a proxy for African data to improve the definition of poorly documented portions of the apparent polar wander (APW) path of Gondwana [7].

In this paper we present paleomagnetic data on strata of latest Ladinian/earliest Carnian age (latest Middle Triassic/earliest Late Triassic; ca. 230 Ma according to the time scale of [8]) from the Al Azizia Formation, belonging to the essentially undeformed Jefara Basin of northwestern Libya. These data are compared with coeval data from the literature from the Southern Alps, with the aim of studying the tectonic relationships between stable Africa and its deformed northern Adriatic margin in the Triassic (Fig. 1). This bridges the gap of data presently existing between substantially concordant Permian and Jurassic/Cretaceous paleomagnetic poles from Africa and Adria. Data from this study and the literature are integrated and a Permian–Cenozoic APW path for Africa/Adria is constructed and discussed from a paleoclimatic and tectonic viewpoint.

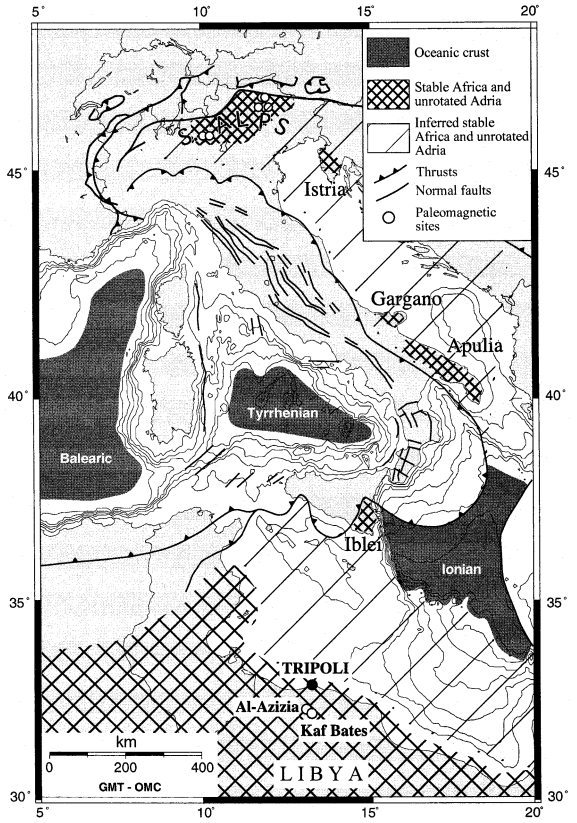

Fig. 1. Simplified tectonic map of the central Mediterranean region with location of Rey paleomagnetic sites.

2. Geology and stratigraphy

Northern Lybia to southeastern Tunisia is one of the few areas in the whole African continent where Permo-Triassic units are exposed. Uplift of the Telemzane Arch, and subsidence along NW/SE-trending grabens in the Jefara Basin at Carboniferous to Early Permian times, was followed by deposition of up to 6 km thick carbonates and locally interbedded bioclastic quartzarenites at Middle to Late Permian times [9,10]. These lagoonal to barrier reef, fusulinid-rich limestones, unconformably overlying older deposits and passing northeastward to deep-marine mudrocks, are beautifully exposed in the Jebel Tebaga (Tunisia), the only marine Permian outcrop in Africa, which we also extensively sampled for paleomagnetic analysis. This Wordian stage of subsidence and transgression is well documented all along the northern margin of Gondwana facing the newly formed Neotethys Ocean [11–13].

Subsidence of the Jefara Basin continued in the Early to Middle Triassic, when alluvial redbeds to marginal marine siliciclastics were deposited [14]. The oldest unit exposed in northwestern Libya is the Kurrush Formation of Ladinian age, consisting of quartzo-feldspathic redbeds including low-grade metamorphic rock fragments and chitinozoans reworked from Devonian mudrocks [15,16]. The intertidal to shallow subtidal, locally cherty carbonates of the overlying Al Azizia Formation, containing brachiopods, pelecypods and gastro-

pods of Early Carnian age (fossil list in [17]), are followed by the varicolored, cross-bedded, marginal marine to braidplain and eolian sandstones of the Abu Shaybah Formation. These quartzarenites to K-feldspar subarkoses, yielding ultrastable dense minerals of bimodal roundness, staurolite, garnet, and opaques, were derived from uplifted areas in the east or southeast, where erosion reached deeper with time into Paleozoic clastics and underlying metamorphic basement rocks [18]. The Jurassic section includes the Abu Ghaylan dolomitic limestones and Bir Al Ghanam evaporites, truncated with angular unconformity by the Lower Cretaceous sedimentary sublitharenites of the Kiklah Formation. Another, major angular unconformity is overlain by quartzose dolomitic limestones representing the base of the Cenomanian Ain Tobi Formation. This relatively undeformed Mesozoic succession is intruded by upper Cenozoic mafic volcanic rocks (see [17] for a geologic map).

2.1. The Al Azizia Formation

The Al Azizia Formation (≥120 m thick) was sampled at two localities: (i) in the stone quarry south of Al Azizia town (on the road from Tripoli to Gharian; 32°32′N, 13°01′E), and (ii) a few kilometers to the southeast at the Kaf Bates hill (32°24′N, 13°07′E). Both localities belong to the Jefara coastal plain, bounded to the north by the Mediterranean sea and to the south by the escarpment of the Tripolitanian Jebel (Jebel Nafusa), a rocky plateau dipping gently towards the Sahara desert.

The 118 m thick Kaf Bates section (Fig. 2) is nearly complete, but the top is not exposed. The upper part of the Kurrush Formation, consisting of very fine- to fine-grained, micaceous, floodplain to upper delta plain redbeds displaying climbing ripples or parallel lamination (~50 m), is sharply overlain by ferruginous stromatolitic limestones and silty limestones, representing the base of the Al Azizia Formation (lithozone A; 4.3 m). The lower part of the formation contains well-bedded limestones, commonly bioturbated or displaying wavy to flaser bedding and rarely hummocky cross-lamination, water escape structures and bioclastic lags; yellowish to reddish, marly interbeds mainly occur at the top of the interval (lithozone B; 89 m), indicating a significant unconformity. The upper part of the formation begins with a marker horizon including very intensely burrowed limestones ('Azizia stone'; lithozone C; 5.9 m), sharply followed by carbonates commonly containing white chert nodules and lenses (lithozone D; ≥19 m).

In the Al Azizia quarry, only the more resistant middle–upper part of the unit is exposed (46 m). The tectonically disturbed basal 24 m were not considered for paleomagnetic study. Sparsely cherty, commonly rippled and bioclastic silty carbonates are capped by a lenticular lithoclastic breccia followed by yellowish silty carbonates and marls (lithozone B; ≥24 m). Next, the 'Azizia stone' marker interval, including very intensely burrowed limestones and reddish marly interbeds (lithozone C; 7.1 m), is followed by gray carbonates with two metric intervals containing lenses of white chert (lithozone D; ≥15 m). The Al Azizia Formation, deposited in lagoonal to tidal flat environments, consists of at least two depositional sequences, each including higher-frequency transgressive/regressive cyclothems (Fig. 2).

2.2. Biostratigraphy

The Al Azizia and Kaf Bates sections have been sampled for pollen and conodont biostratigraphy (Fig. 2). Only two pollen samples at Al Azizia yielded valid biostratigraphic information. Sample Lyt 152 is dominated by large equidimensional particles of inertinite and pyrite, with subordinate, small-sized vitrinite debris. The only sporomorph is *Enzonalasporites vigens*, indicating a Ladinian/Carnian age. The overlying sample Lyt 151 contains a low amount of organic matter mostly consisting of small equidimensional inertinite and subordinate vitrinite debris. Palynomorphs include rare *Enzonalasporites vigens*, *Patinasporites densus*, *Duplicisporites granulatus*, *Duplicisporites* sp., *Gordonispora fossulata*, *Aratrisporites fimbriatus*, *Aratrisporites* sp., *Retitriletes* sp. and *Sellaspora foveorugulata*. Bisaccates include *Cuneatisporites* sp., *Platysaccus* sp., *Alisporites* sp., *Schizosaccus* sp. and *Ovalipollis pseudoalatus*.

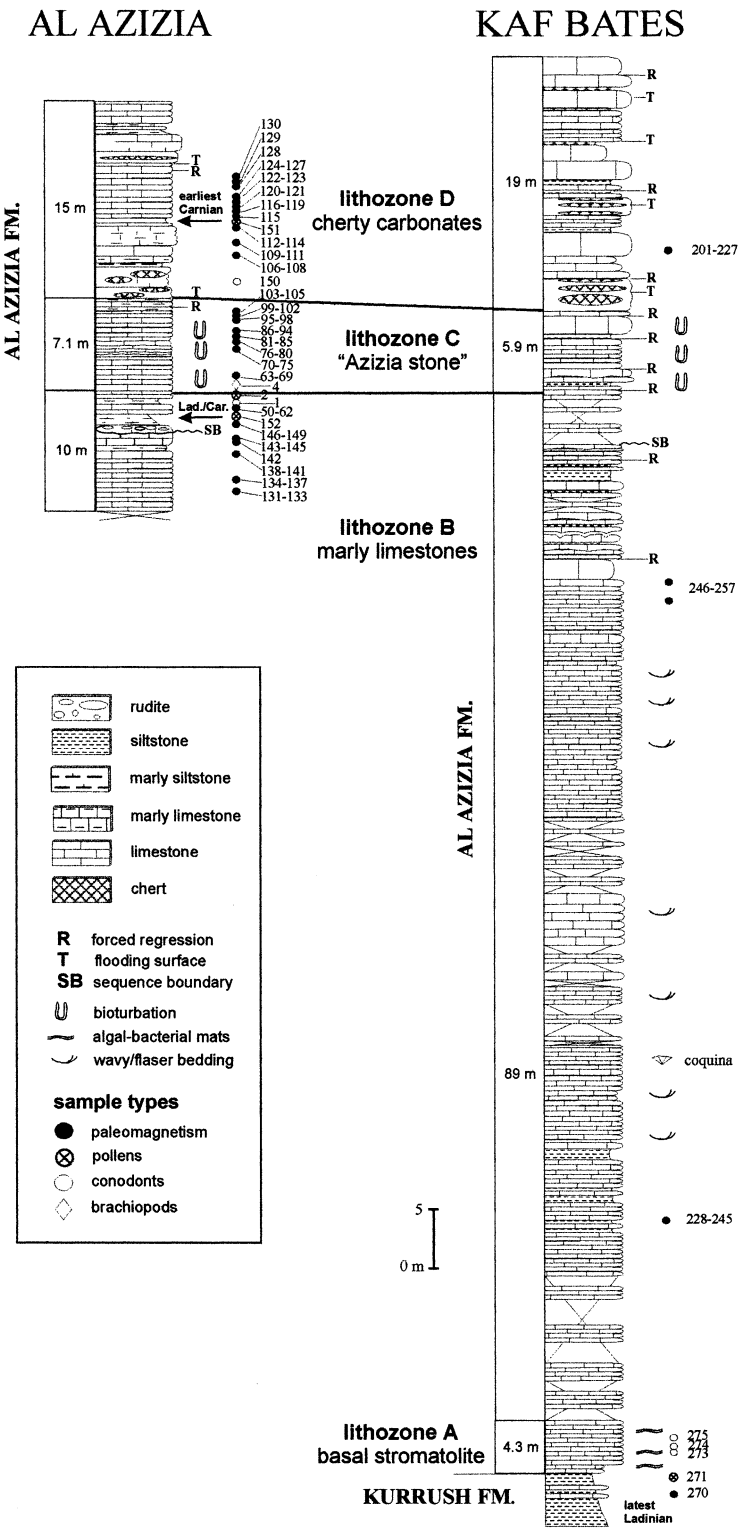
AL AZIZIA
KAF BATES
AL AZIZIA FM.
15 m
7.1 m
10 m
earliest Carnian
Lad./Car.
SB
T
R
130
129
128
124-127
122-123
120-121
116-119
115
151
112-114
109-111
106-108
150
103-105
99-102
95-98
86-94
81-85
76-80
70-75
63-69
4
2
1
50-62
152
146-149
143-145
142
138-141
134-137
131-133
lithozone D
cherty carbonates
lithozone C
"Azizia stone"
lithozone B
marly limestones
lithozone A
basal stromatolite
KURRUSH FM.
19 m
5.9 m
89 m
4.3 m
201-227
246-257
228-245
coquina
275
274
273
271
270
latest Ladinian
5
0 m
rudite
siltstone
marly siltstone
marly limestone
limestone
chert
R forced regression
T flooding surface
SB sequence boundary
bioturbation
algal-bacterial mats
wavy/flaser bedding
sample types
paleomagnetism
pollens
conodonts
brachiopods

Fig. 2. The latest Ladinian/earliest Carnian Al Azizia and Kaf Bates sections of the Al Azizia Formation, sampled for paleomagnetic and biostratigraphic analysis. The unit displays two transgressive–regressive cycles (depositional sequences *sensu* [43], with transgressive systems tracts represented by lithozones A and D. The lower boundary with the Kurrush Formation is a transgressive surface. Lithozone B is interpreted as an highstand systems tract and lithozone C as a shelf-margin wedge. The sequence boundary, marked by a lenticular lithoclastic breccia, roughly corresponds to the Ladinian/Carnian boundary. Higher-frequency (Milankovian?) parasequences, separated by discontinuity surfaces, are also recognized.
←

This association is ascribed to the upper part of the *secatus–vigens* phase of earliest Carnian age [19].

Most samples from the underlying Kurrush Formation contain minor preserved organic matter and no palynomorphs. Only sample Lyt 156, collected at the core of the Gharian dome, yielded brown vitrinite, sporomorphs, fungal remains, and minor inertinite. Sporomorphs include *Camerosporites secatus*, *Partitisporites tenebrosus*, *Nevesisporites vallatus*, *Calamospora* sp., *Ephedripites primus*, *Cycadopites* sp., *Duplicisporites granulatus*, *Duplicisporites* sp., *Retitriletes* sp., *Gordonispora fossulata*, *Foveosporites visscheri* and *Aratrisporites* sp. Most representative bisaccates are *Staurosaccites quadrifidus*, *Infernopollenites parvus*, and rare *Ovalipollis pseudoalatus*. Due to association of *C. secatus* with some late Ladinian index taxa (i.e., *N. vallatus*, *G. fossulata*, *F. visscheri*), considered to disappear in the upper part of the early Carnian *vigens–densus* phase [19,20], this assemblage from the Kurrush Formation may be ascribed to the latest Ladinian (uppermost part of *secatus–dimorphus* or *secatus–vigens* phase of [19]).

In conclusion, the Al Azizia Formation is comprised in age between the latest Ladinian (i.e., the palynological age of the underlying Kurrush Formation) and the earliest Carnian (i.e., the palynological age of the upper Al Azizia Formation at Al Azizia) (Fig. 2).

3. Paleomagnetism

The paleomagnetism of the Al Azizia Formation at Al Azizia and Kaf Bates has been previously studied by Martin et al. [21]. These authors were unable to isolate a characteristic component of magnetization because the magnetization intensity was too low for the Schonstedt magnetometer at their disposal.

3.1. Paleomagnetic techniques

A total of 99 field cores (109 standard 11.4 cm^3 specimens) and 56 field cores (68 standard 11.4 cm^3 specimens) were collected with a water-cooled rock drill in the uppermost Ladinian/lowermost Carnian limestones of the Al Azizia Formation at Al Azizia and Kaf Bates, respectively (Fig. 2), and oriented with a magnetic compass. The natural remanent magnetization (NRM) of all specimens was measured on a 2G Enterprises DC-squid cryogenic magnetometer at the paleomagnetic laboratory of ETH Zürich. After pilot AF and thermal demagnetization, specimens were thermally demagnetized in 50–20°C steps up to a maximum of 670°C in a magnetically shielded oven. Rock magnetic properties were studied at the Istituto Nazionale di Geofisica e Vulcanologia in Rome. Nine representative specimens were given a composite IRM by imparting 2.7, 0.6 and 0.12 T fields along specimen *z*-, *y*- and *x*-axes, respectively, with a 2G Enterprises pulse magnetizer. This composite IRM was thermally demagnetized in 50°C steps up to 700°C [22] in order to determine the magnetic mineralogy content of the Al Azizia Formation. Hysteresis properties and susceptibility variations during heating–cooling cycles were determined with a Molspin VSM magnetometer and an AGICO CS3 system, respectively. Principal component analysis [23] was applied to determine the component directions of NRM, chosen by inspection of vector end-point demagnetization diagrams [24]. Site mean directions were determined using standard Fisher statistics.

3.2. Rock magnetic properties

The mean NRM intensity is 0.94 mA/m at Al Azizia and 2.3 mA/m at Kaf Bates and drops on average by 75% at both sites upon heating at

120°C. Thermal unblocking characteristics of orthogonal axis IRM [22] show that the samples are dominated by a high coercivity phase characterized by maximum unblocking temperatures of about 120°C, interpreted as goethite (Fig. 3). This main magnetic phase is followed at higher temperatures by a low coercivity component with maximum unblocking temperatures around 500°C and a high coercivity phase with maximum unblocking temperatures around 650°C. These components are interpreted as titano-magnetite and hematite, respectively. Hysteresis properties and susceptibility variations upon heating and cooling confirm the presence of a mixed mineralogy with contrasting coercivity.

3.3. Paleomagnetic directions

An initial 'A' component of magnetization consistent with viscous acquisition along the present-day field direction was thermally unblocked between room temperature and a mean of 200°C in 58% of the specimens from Al Azizia and

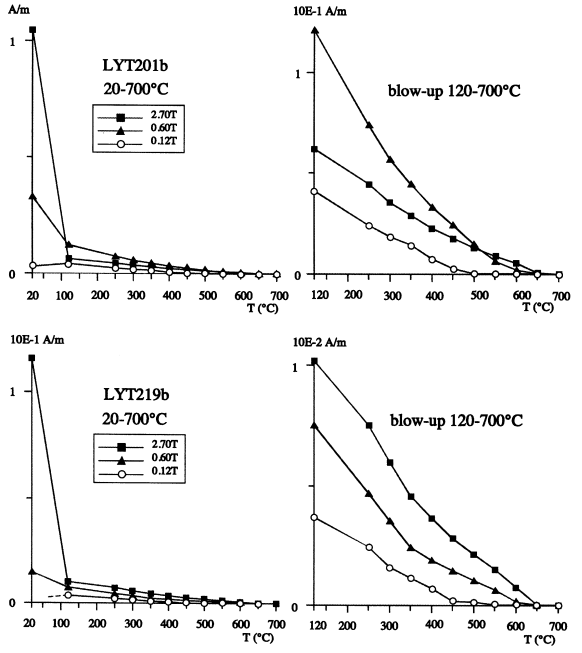

Fig. 3. Thermal unblocking characteristics of orthogonal axis IRMs [22] for representative samples of the Al Azizia Formation. Demagnetization steps in °C.

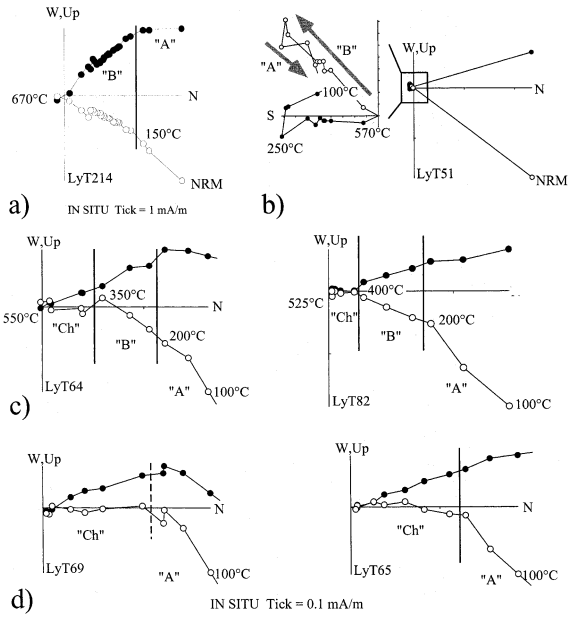

Fig. 4. Zijderveld thermal demagnetograms of NRM of representative samples from the Al Azizia section of the Al Azizia Formation. Closed symbols are projections onto the horizontal plane and open symbols are projections onto the vertical plane in in situ coordinates. Demagnetization steps in °C. See text for discussion.

70% of the specimens from Kaf Bates (Fig. 4). A 'B' component exhibiting both polarities was isolated to the origin in 31% (Al Azizia) and 82% (Kaf Bates) of the specimens in the mean temperature range between 200 and 500°C up to a maximum of 670°C. These directions are oriented north-northwesterly with positive inclinations (Fig. 4a) or southerly with negative inclinations (Fig. 4b). This 'B' component of magnetization is occasionally accompanied by a shallower, northerly characteristic ('Ch') component isolated between about 400 and 500°C up to a maximum of 550°C (Fig. 4c). More commonly, the 'Ch' component directly follows the present-day field direction from about 300 to 500°C up to a maximum of 550°C (Fig. 4d). The 'Ch' component has been successfully retrieved in 40% of the specimens at Al Azizia and 36% of the specimens at Kaf Bates (Table 1). We observe that the 'B' component of magnetization is sometimes associated with maximum unblocking temperatures consistent with those expected for hematite (e.g.,

Fig. 4a), whereas the 'Ch' component unblocking temperatures never exceed those expected for magnetite.

The 'A' and 'B' components are interpreted as more steeply inclined overprints, whereas the 'Ch' component is considered the original latest Ladinian/earliest Carnian magnetization acquired in the northern hemisphere [6] during a period of predominant normal polarity, in broad agreement with normal polarity-dominated data from other Ladinian/Carnian boundary sections from the literature ([20] and references therein).

The Al Azizia paleomagnetic directions do not vary appreciably in orientation upon correction for bedding tilt because the attitude of beds at both sites is virtually horizontal (Fig. 5a,b; Table 1).

3.4. Paleomagnetic poles

The 'Ch' magnetization component from Al Azizia and Kaf Bates yields statistically indistinguishable paleomagnetic poles which lie, in tilt-corrected coordinates, at 214°E/59°N and 226°E/54.5°N, respectively (Table 1). The latest Ladinian/earliest Carnian Al Azizia poles also compare closely with coeval Ladinian/Carnian paleomagnetic poles from the Southern Alps from the literature (Table 2).

Unlike the Apennines, significant differential rotation of thrust sheets in the Southern Alps is restricted to the immediate vicinity of major faults (e.g., Insubric, Giudicarie and Valsugana Line). Crustal deformation is particularly low in the Dolomites, where most of the data come from, and the rigid 1.7 km thick Permian porphyrites underlies the Mesozoic sedimentary sequence. Paleomagnetic investigations on the Triassic of the Southern Alps (Fig. 1; Table 2) show that deformation was essentially cylindrical: after application of bedding tilt correction, data from outcrops even hundreds of kilometers apart converge (Fig. 6a,b). At full (100%) tilting correction, the seven Southern Alps poles pass the fold test [25] at the

Table 1
Paleomagnetic directions and paleopoles from the Al Azizia Formation

Locality	Coordinates	Comp.	% Normal	N_1/N_2	In situ				Tilt-corrected			
					Dec.	Inc.	k	α_{95}	Dec.	Inc.	k	α_{95}
Al Azizia	32.5°N, 13.2°E	'A'	100	058/109	355.5	45.6	26	3.7	000.1	50.4	25	3.8
Kaf Bates	32.4°N, 13.1°E	'A'	100	039/068	358.6	45.6	36	3.9	012.7	28.1	22	5.0
Al Azizia		'B'	68	019/109	349.2	30.8	22	7.3	350.7	35.9	21	7.4
Kaf Bates		'B'	91	046/068	327.7	38.9	12	6.4	343.6	36.9	17	5.3
Al Azizia		'Ch'	100	040/109	349.0	1.5	35	3.9	349.5	6.9	36	3.8
Kaf Bates		'Ch'	100	020/068	339.0	7.9	25	6.7	341.7	2.7	36	5.5

		In situ			Tilt-corrected			paleolatitude
		Long.	Lat.	dp/dm	Long.	Lat.	dp/dm	
Al Azizia	'A'	229.9	83.3	3.0/4.7	189.6	88.6	3.4/5.1	27 (±3)
Kaf Bates	'A'	206.3	84.5	3.2/5.0	156.6	69.1	3.0/5.5	27 (±3)
Al Azizia	'B'	227.3	71.3	4.5/8.1	228.9	74.9	5.0/8.6	20 (±5)
Kaf Bates	'B'	271.2	59.6	4.5/7.6	248.2	71.2	3.6/6.2	21 (±4)
Al Azizia	'Ch'	213.5	56.6	2.0/3.9	214.1	59.3	1.9/3.9	3.5 (±2)
Kaf Bates	'Ch'	232.2	55.4	3.4/6.7	225.8	54.5	2.8/5.5	1 (±3)

Comp.: magnetization component; % Normal: percentage of samples bearing normal polarity; N_1: number of the paleomagnetic directions used to calculate the mean; N_2: total number of standard 11.4 cm^3 specimens; Dec., Inc.: declination and inclination; k: Fisher precision parameter; α_{95}: Fisher radius of cone of 95% confidence about the mean direction; Long., Lat.: longitude and latitude of paleomagnetic pole; dp/dm confidence oval about the paleomagnetic pole. The paleolatitude is calculated in in situ coordinates for the 'A' component, and tilt-corrected coordinates for the 'B' and 'Ch' components, and is expressed in degrees north of the equator. Bedding attitude, expressed as azimuth of bedding dip vs. angle of dip, is 140°E/10° at Al Azizia and 50–180°E/10–14° at Kaf Bates.

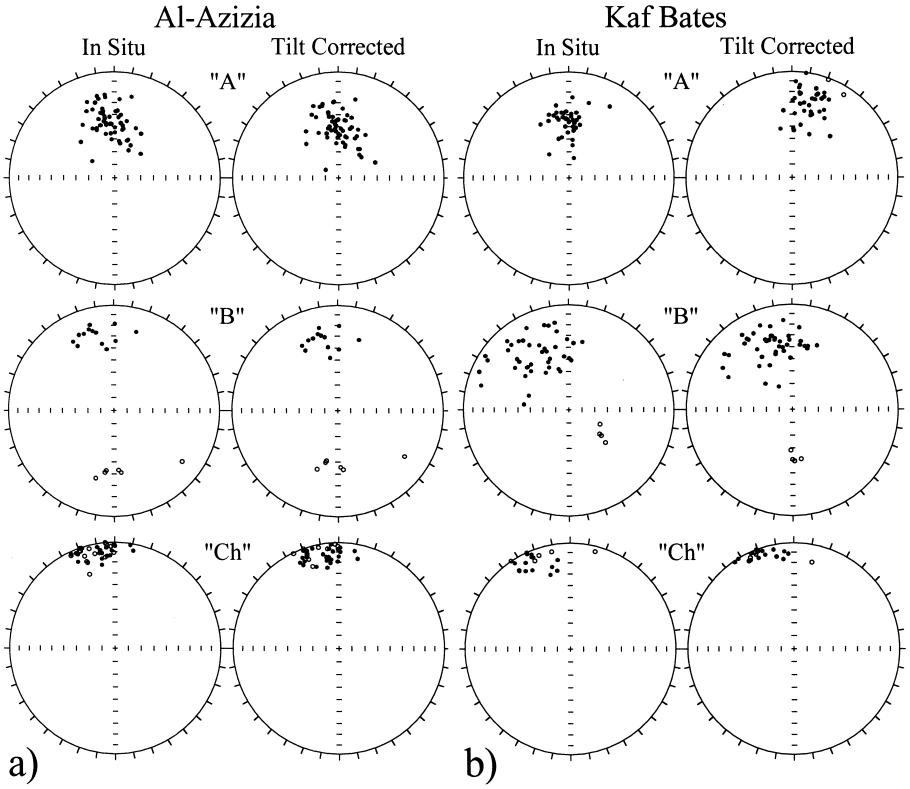

Fig. 5. Equal area projections before (in situ) and after bedding tilt correction of the 'A', 'B' and characteristic 'Ch' component directions from (a) the Al Azizia and (b) the Kaf Bates section of the Al Azizia Formation.

95% level of confidence (Fig. 6c). Some small-scale rotations of thrust sheets, however, cannot be ruled out and may partly account for data scattering (Fig. 6a,b). The peak in grouping at around 80% unfolding (Fig. 6c) is probably an artefact of unrecognized or incomplete correction for tilting at one or more sites. We infer that eastern Southern Alps paleomagnetic data are primary in age and must therefore be looked at after full (100%) correction for tilting, rather than at any intermediate percentage of unfolding. Robust magnetostratigraphic cross-correlations confirm the primary age of the remanence acquisition at Southern Alps Triassic sections [26]. The latest Ladinian/earliest Carnian Al Azizia poles at 100% unfolding coincide with the Ladinian/Carnian overall paleomagnetic pole from the Southern Alps at similar unfolding correction (Fig. 6d), supporting a substantial tectonic coherence of Africa and Adria during Triassic times.

4. Adria as Africa's adjunct unit

The hypothesis that Adria is an adjunct unit of Africa is also supported by data from the Early Permian, Late Jurassic/Early Cretaceous, and Late Cretaceous (Fig. 7a) from Adria and West Gondwana (Fig. 7b). Early Permian paleomagnetic poles from the Southern Alps [7], and coeval poles from Africa [4] (Fig. 7b), coincide within the uncertainties associated with both datasets when viewed in northwest Africa coordinates (eP in Fig. 7a). Late Jurassic/Early Cretaceous and Late Cretaceous paleopoles from the Southern Alps, Istria, Apulia, Gargano and Iblei [3] are internally consistent, suggesting that these regions of Adria moved in close mutual conjunction. The Late Jurassic/Early Cretaceous paleopoles coincide with coeval top-quality poles from the Ithaca (USA) and Swartruggens (South Africa) kimberlites [27,28], and the Late Cretaceous paleopoles agree

with Late Cretaceous West Gondwana poles [4] rotated into northwest Africa coordinates (lJ/eK and lK in Fig. 7a, respectively). It therefore appears that Adria constitutes a single unit which followed the main movements of the African plate since at least Early Permian times.

Critical to this reconstruction model is the 330 km wide Ionian ocean, located between Apulia and the Iblei/Africa margin (Fig. 1). It is yet unknown whether the Ionian seaway, originated at Permian to early Mesozoic times [29–31], is underlain by thinned continental crust or, rather, is an aborted, dormant ocean basin. Its original northwestward extension is also undetermined, due to Cenozoic subduction beneath the Apennine front. A model recently presented by [31] hypothesizes a continuation of the Mesozoic Ionian ocean toward the west/northwest, cutting trough early Mesozoic paleogeography and separating Iblei/north Africa from Apulia (Fig. 8a). The separation of Adria from Iblei/Africa that it should have induced is not resolvable with the available paleomagnetic database, and cannot in any case be accounted for by an Euler pole of opening located on or close to Adria.

We envisage herein an alternative paleogeographic scenario at Paleogene times depicting instead Adria as a Florida-type promontory of Africa, with broadly continuous north–south paleogeographic trends from Tunisia to the Southern Alps, and confined to the west by the Mesozoic Ligurian ocean and to the southeast by the Ionian ocean (Fig. 8b). Apennine orogeny proceeded from the west to the east, so that eastern, more external portions of Adria (i.e., Istria, Gargano, Apulia and Iblei) survived severe deformation. This reconstruction is consistent with: (i) long-established identity within error resolution of a few degrees of Permo-Mesozoic paleomagnetic poles from Africa and Adria; (ii) lack of subduction of the Ionian west/northwest prolongation in Alpine times in spite of continuous north/south convergence between Africa and Europe since the Late Cretaceous; (iii) occurrence of Mid-Tertiary African-derived Numidian

Table 2
Middle–Late Triassic paleomagnetic poles from the Southern Alps

	Rock unit	Locality	Coordinates	In situ				Tilt-corrected					Reference
				Long.	Lat.	dp/dm		Long.	Lat.	dp/dm			
1	Buchenstein Beds	Belvedere (Dolomites)	46.4/12.0	284	69	09/12		217	52	04/08			[26]
2	Buchenstein Beds	Pedraces (Dolomites)	46.6/11.9	197	25	08/14		223	69	10/15			[26]
3	Buchenstein Beds	Frötschbach (Dolomites)	46.6/11.8	221	56	03/06		211	64	04/07			[44]
4	S. Cassiano Fm.	Stuores (Dolomites)	46.6/11.9	187	66	04/07		193	52	03/06			[20]
5	Lad.-Car. volc.	Dolomites	46.4/11.7	242	50	06/10		240	48	05/10			[45]
6	V. Scalve porph.	Lombardy	45.8/10.2	258	69	06/08		221	52	03/06			[46]
7	V. Sabbia Ss.	Lombardy	45.8/10.0	210	57	12/23		215	57	08/14			[7]
				Long.	Lat.	k_1	α_{95}	Long.	Lat.	k_2	α_{95}	k_2/k_1	Paleo-lat.[a]
All $n=7$				221	60	13	17	217	57	53	8	4	15.5°N

Long., Lat.: longitude and latitude of paleomagnetic pole; dp, dm: semi-axes of the confidence oval about the paleomagnetic pole. k_1, k_2: Fisher precision parameters before and after bedding tilt correction, respectively; α_{95}: Fisher half-angle of cone of 95% confidence about the paleomagnetic pole.

[a]Calculated at a point located at 46.2°N, 11.5°E (southern Dolomites).

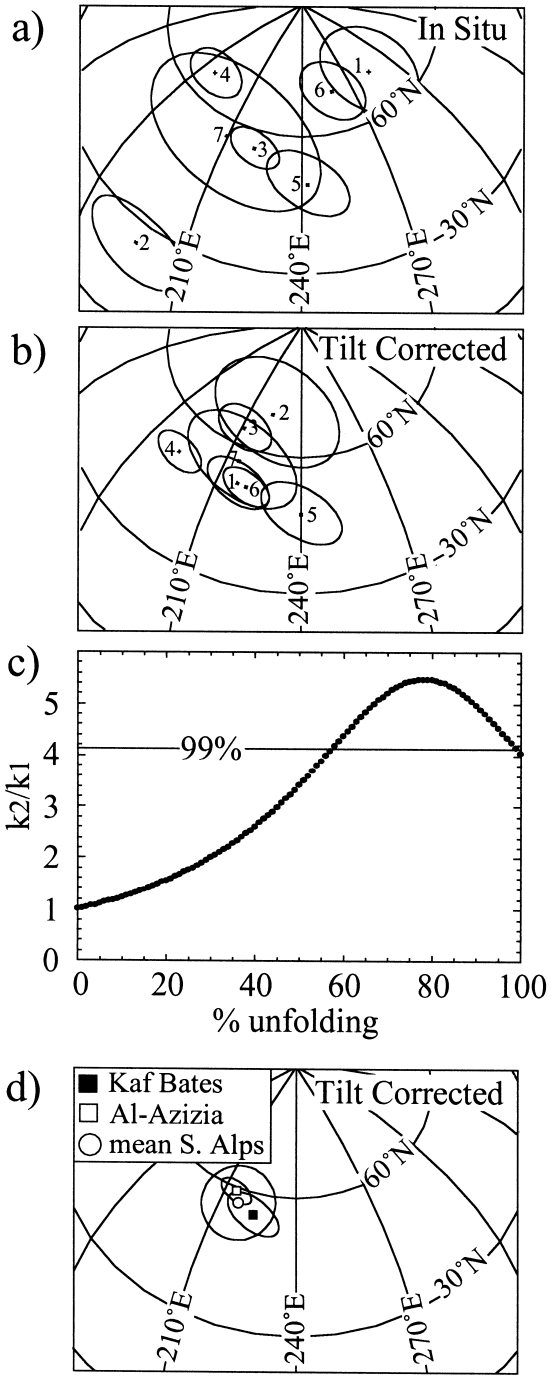

Fig. 6. Projections (a) before and (b) after bedding tilt correction of late Middle Triassic to early Late Triassic paleomagnetic poles from the Southern Alps (Table 2). (c) Variation of Fisher precision parameter k upon bedding tilt correction for the Southern Alps paleopoles. (d) Comparison between the Southern Alps overall mean paleopole and coeval paleopoles from Al Azizia and Kaf Bates (Table 1). See text for discussion.

←

'flysch' both in Sicily and in the southern Apennines [32], which is difficult to reconcile with the presence of the Ionian west/northwest prolongation separating these two regions.

5. Construction of the Africa/Adria APW path

We integrate data from Adria and West Gondwana in northwest African coordinates (Table 3) to construct a composite APW path from the Early Permian to the Pliocene (Fig. 9). The Permian–Triassic portion of the curve is upgraded from Muttoni et al. [7]; the Mesozoic portion of the curve is essentially derived from Channell [3] and Van der Voo [4], whereas Cenozoic data come from deep-sea drill cores taken at different localities on the African plate [33,34]. This curve compares with the previously published APW path of Besse and Courtillot [35], apart from sensible departures in the Jurassic, mid-Cretaceous and Eocene–Oligocene (Fig. 10a).

The Permian–Triassic segment of the APW path of this study corresponds to Pangea northward motion and counter-clockwise rotation at an overall plate speed of 4–10 cm/yr (Fig. 10b–e). The Jurassic segment of the loop corresponds instead to the opening of the Central Atlantic ocean between North America and Africa in the Middle Jurassic, which caused Africa/Adria to drift towards southern latitudes and to rotate clockwise; plate motion took place at an overall speed of about 7 cm/yr. Finally, the Cretaceous portion of the loop tracks an increase in Africa/Adria latitude and counter-clockwise rotation during opening of the Southern Atlantic, prior to final north/south convergence with Eurasia in the Cenozoic at the time of opening of the Labrador/Northern Atlantic oceans.

6. Paleoclimatic interpretation

Useful paleoclimatic information can be obtained from the Africa/Adria APW path by super-

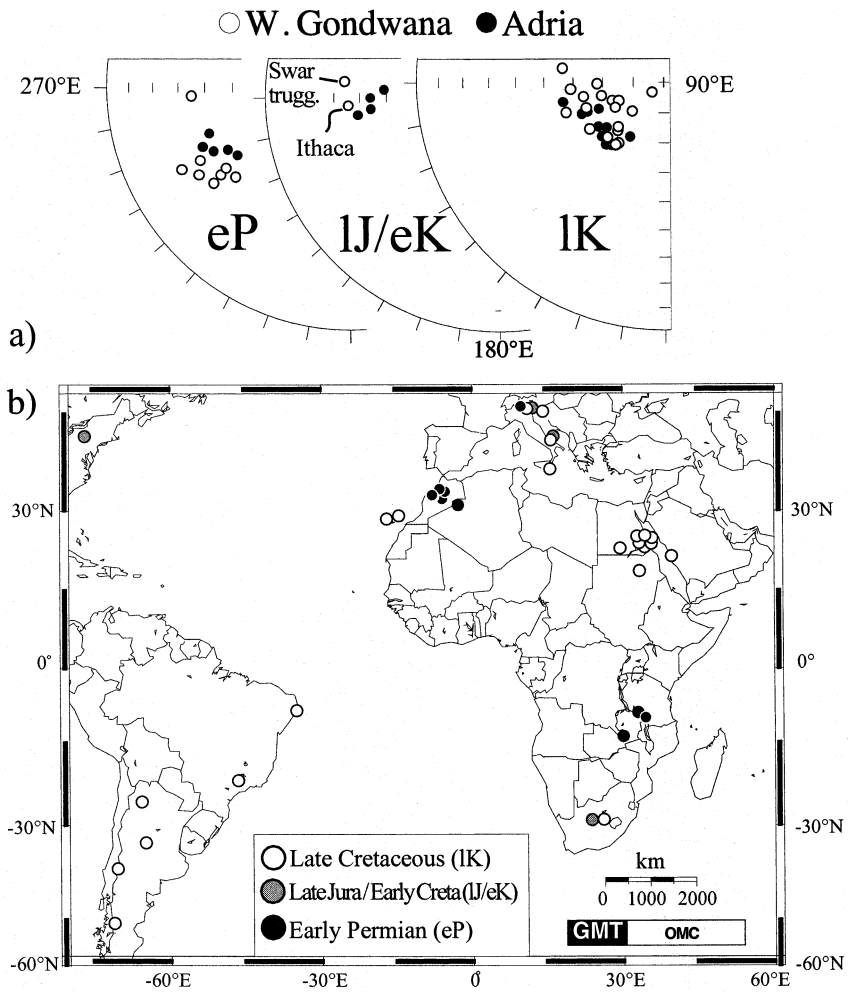

Fig. 7. (a) Equal area projections after bedding tilt correction of mean paleomagnetic poles from Adria (solid dots) and West Gondwana (empty dots) in northwest African coordinates for the Early Permian, Late Jurassic/Early Cretaceous and Late Cretaceous. (b) Geographic location of paleomagnetic data of Early Permian to Late Cretaceous age from Adria and West Gondwana. The pole of the Late Jurassic/Early Cretaceous Ithaca (USA) kimberlite [27] is also shown.

posing the expected paleolatitude trend for a nominal point located, for example, in northern Libya (e.g., 32.5°N, 13°E) on zonal latitudinal climatic bands (Fig. 10b). The zonal mean annual averages of evaporation (E) and precipitation (P) and their relative variations (E-P rate [36]) are important elements of climate and hydrology. The measured E-P values in modern-day climate show an excess of precipitation over evaporation at middle and high latitudes as well as in the equatorial zone between 10°N and 10°S, whereas a deficit of precipitation is found in the subtropical regions between about latitudes 10° and 35°. Such a modern zonal climate model, found to be valid for the Late Triassic of North America [37], constitutes a useful null hypothesis for understanding the distribution of paleoclimate proxies. Inspection of Fig. 9b suggests that northern Libya moved progressively northward over the period of existence of Pangea, and crossed the boundary between the humid equatorial and the arid tropical belt sometimes in the Late Triassic. From the Jurassic onwards, northern Libya remained in the arid tropical belt.

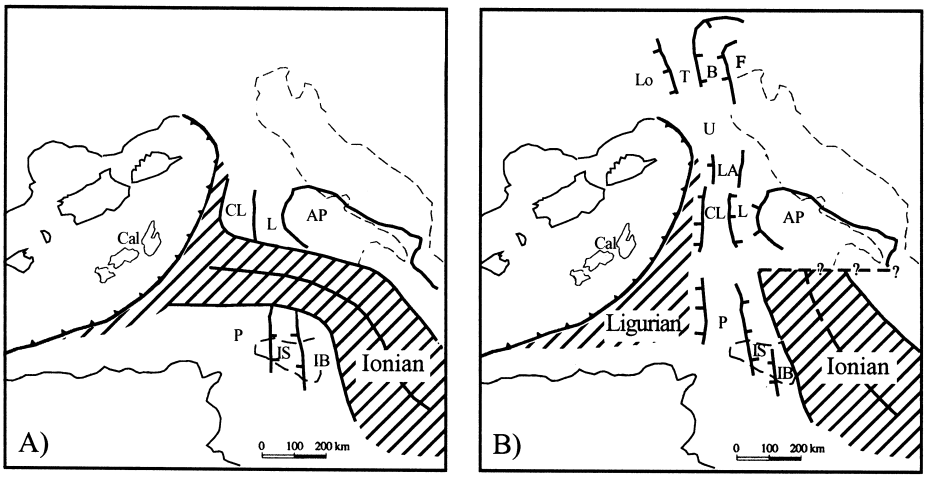

Fig. 8. Alternative solutions for central Mediterranean paleogeography at Paleogene times. (a) The model recently presented by Catalano et al. [31] hypothesizes continuation of the Mesozoic Ionian ocean toward the west/northwest, cutting through early Mesozoic paleogeography and separating north Africa from Apulia. (b) The tentative model presented herein depicts Adria as a Florida-type promontory of Africa, with broadly continuous north–south structural trends from Tunisia to the Southern Alps. AP = Apulia–Gargano platform, B = Belluno basin, Cal = Calabria block, CL = Campano–Lucana platform, F = Friuli–Istria platform, IB = Iblei platform, IS = Imerese–Sicani basins, L = Lagonegro basin, LA = Laziale–Abruzzese platform, Lo = Lombard basin, U = Umbria–Marche basin, P = Panormide platform.

Table 3
Adria and West Gondwana paleopoles

Name	Age (Ma)	Age (relative)	Lat. (°N)	Long. (°E)	k	α_{95} dp/dm	N	Locality	Reference
eP	285	E. Permian	36.2	243.3	77	4.8	13*	AF, SAP	[7]
lP/eTr	250	L. Permian/ E. Triassic	46.8	237.6	317	3.1	8*	SAP	[7]
mTr/eTrl	233	M./early L. Triassic	57.1	218.1	67	6.3	9*	AF, SAP	this study
lTr/eJ	202	L. Triassic/ E. Jurassic	71.1	214.8	458	4.3	4*	AF	[7]
eJ	191	E. Jurassic	72.0	248.5	108	4.7	10*	AF	[4]
lJ/eK	144	L. Jurassic/ E. Cretaceous	40.8	269.2	125	6.0	6*	AF, NAM, SAP, G, U	[3,27,28] combined
mK_1	99	M. Cretaceous	46.8	262.9	42	4.9/8.1	12§	AP	[47]
mK_2	99	M. Cretaceous	52.0	257.0		3.7/6.2		SA	[3]
lK	82	L. Cretaceous	66.6	241.5	71	3.2	29*	AF, SAM, SAP, IS, G, IB, U	[3,4] combined
Pa	60	Paleocene	70.1	213.0		2.4/4.4		AF	[34]
E	44	Eocene	69.0	189.0		5.8		AF	[33]
O	29	Oligocene	75.9	193.0		2.0/4.4		AF	[34]
M	14	Miocene	81.0	154.0		5.6		AF	[33]
P	3	Pliocene	86.0	149.0		2.6		AF	[33]

Age (Ma): mean age of paleopoles in millions of years according to the time scale of [8]; Lat., Long.: paleopole coordinates; k, α_{95}, dp/dm: paleopole statistics; N: number of overall mean (*) or site mean (§) directions used to calculate the paleopole. AF = Africa, SAM = South America, NAM = North America (Ithaca kimberlite [27]), SAP = Southern Alps, IS = Istria, G = Gargano, AP = Apulia, IB = Iblei, U = NW Umbria, corrected for Apennine rotation (see [3]).

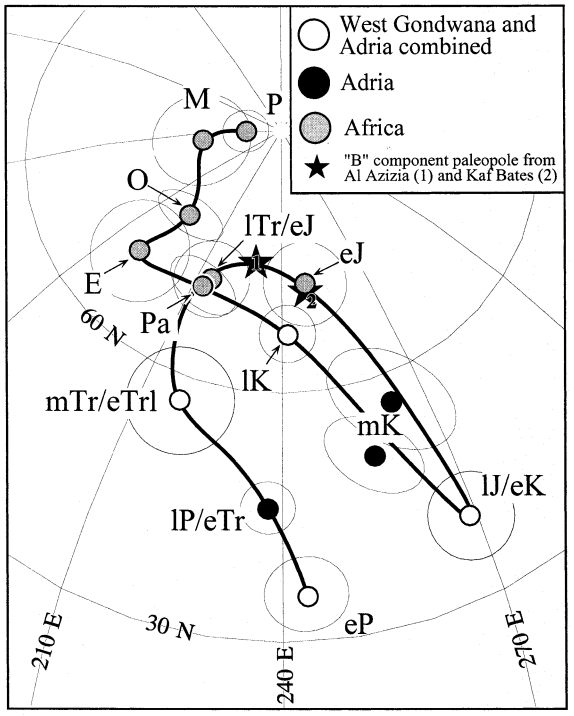

Fig. 9. Composite APW path for Africa/Adria. Mean poles are taken from Table 3; eP = Early Permian, lP/eTr = Late Permian/Early Triassic, mTr/eTrl = Middle Triassic/early Late Triassic, lTr/eJ = Late Triassic/Early Jurassic, eJ = Early Jurassic, lJ/eK = Late Jurassic/Early Cretaceous, mK = middle Cretaceous, lK = Late Cretaceous, Pa = Paleocene, E = Eocene, O = Oligocene, M = Miocene and P = Pliocene.

Palynofacies and microflora analysis from this study and the literature from northeastern Libya and southeastern Tunisia [14,38] confirms this trend, as discussed below:

1. In the Upper Permian, a warm and humid climate is indicated by xerophytic elements (*sensu* [39]) such as bisaccate, striate, and taeniate pollen forms (*Lueckisporites Taeniasporites*), associated with hygrophytic elements such as monosulcate pollens (*Cycadopites*), monolete spores (*Punctatisporites*), pollens derived by seed ferns (*Platysaccus*), and rare pteridophytes (*Lundbladispora*). In Tunisia, transition from dominant carbonates with intercalated anhydrites and siliciclastics in the mid-Permian to siliciclastics with wood logs in the uppermost Permian [10] suggests a progressive increase in humidity during northward latitudinal drift toward the equator.
2. In the Early Triassic, more humid conditions are indicated by the predominance of hygrophytic elements such as microspores of lycopodiophytic affinity (*Endosporites*, *Densoisporites*), spores produced by ferns and other Filicinae (*Apiculatisporites*, *Deltoidospora*) and Equisetites (*Calamospora*, *Retusotriletes*), in association with less abundant bisaccate taeniate pollens (*Taeniasporites*). This assemblage is typical of lowland floodplains and marshes dominated by hydrophilic and mesophilic pteridophytes and pteridosperms, possibly with locally drier environments supporting xerophilic and mesophilic conifers and pteridosperms. Subequatorial latitudes are also suggested by dominant redbeds with laterite concretions in Tunisia.
3. In the Middle–early Late Triassic, a drier climate is suggested by abundance of xerophytic elements in the Kurrush and overlying Al Azizia Formation, including circumpolloid (*Duplicisporites*, *Partitisporites*, *Camerosporites*), monosaccate (*Enzonalasporites*, *Patinasporites*), and subordinate polyplicate pollens (*Ephedripites*). Rare lycopod cavate monolete microspores (*Aratrisporites*) and monosulcate pollens (*Cycadopytes*) suggest local conditions characterized by river water supply which promoted the growth of such hygrophytic plant communities on the coastal plain. Similar microfloras, with abundant and diversified xerophytic indicators (*Triadispora complex*, circumpolloids), were collected in Tunisia and from exploration wells in northern Lybia [14,38].
4. In the Late Triassic, an arid/semiarid, subtropical climate is indicated by dominant xerophytic microflora. Marginal marine carbonates and evaporites to wadi and eolian clastics in central Tunisia to northern Libya [18,38,40,41] confirm this trend toward increasingly arid conditions at the close of the Triassic.
5. In the Jurassic, tropical arid settings are testified by the Abu Ghaylan sabkha dolomites and Bir Al Ghanam evaporites of northern Libya (Fig. 10b).

7. Conclusions

Relatively unrotated regions of Adria moved in close conjunction with Africa since Permian times. Adria data can thus be used to improve the definition of the Africa reference APW path for paleogeographic map generation. The Africa/Adria APW path presented here confirms previous interpretations regarding Pangea configuration and evolution at Triassic times [7]. This composite APW path may also be used to quantify thrust sheet rotations within Africa deformed and rotated margins (e.g., the Apennines), or date primary and secondary magnetizations in case more stringent geological information is lacking. For example, the 'B' magnetization component from the Al Azizia Formation, yielding paleomagnetic poles located above 70°N in tilt-corrected coordinates (where grouping is best; Table 1), may be interpreted by inspection of Fig. 9 as due to a remagnetization event of Early Jurassic age, i.e., coeval to the opening of the Central Atlantic/Ligurian ocean.

The zonal latitudinal bands of relative aridity and humidity typical of modern-day climate superposed to the paleolatitude trend for northern Libya predict that northern Libya crossed the humid subequatorial/arid subtropical boundary zone at Late Triassic times. This inference is fully supported by Permo-Triassic palynological and facies analysis from this study and the literature. We conclude that a zonal climate model coupled with paleomagnetically constrained paleogeographic reconstructions indeed provides a powerful null hypothesis for understanding past climatic conditions. It should be noted, however, that this zonal configuration of relative humidity and aridity may be subject to considerable modifications in response to large-scale geologic events. For example, igneous superactivity is thought to be responsible for widespread greenhouse conditions in the mid-Cretaceous [42] at latitudes compatible with the zonal arid tropical belt.

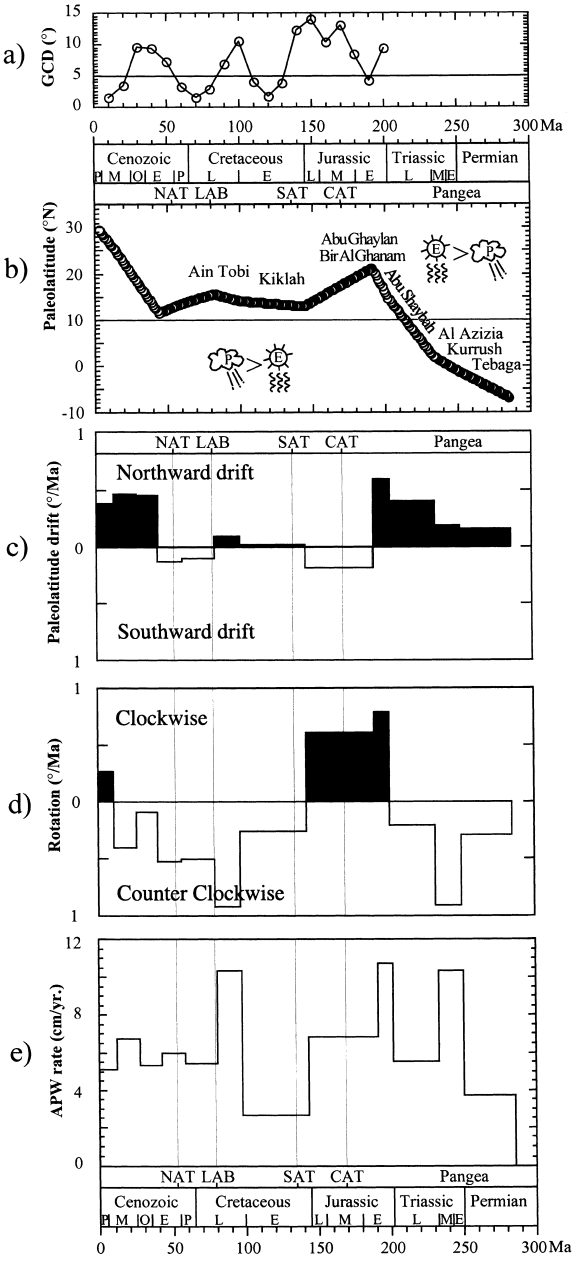

←

Fig. 10. (a) Great circle distance between the composite Africa/Adria APW path of this study and the master APW path of [35] in African coordinates. (b–d) Paleolatitude (b), latitudinal drift (c), and rate of angular rotation (d) calculated for a point in northern Libya located at 32.5°N, 13°E from the Africa/Adria APW path of this study. (e) Rate of APW, which combines the effects of continental drift and true polar wander, and is independent of geographic location. CAT = Central Atlantic opening, SAT = Southern Atlantic opening, LAB = Labrador sea opening, NAT = Northern Atlantic opening.

Acknowledgements

The authors wish to thank Franco Sirtori, AGIP, Tripoli, and Osama and Tarek Ellali for technical assistance in Libya. The manuscript greatly benefitted from careful reviews by Fabio Speranza and Dennis V. Kent, and from discussion with Maurizio Gaetani, Carlo Doglioni, and Mario Fornaciari.*[RV]*

References

[1] J.E.T. Channell, B. D'Argenio, F. Horvath, Adria, the African promontory, in Mesozoic Mediterranean palaeogeography, Earth Sci. Rev. 15 (1979) 213–292.

[2] W. Lowrie, Paleomagnetism and the Adriatic promontory: a reappraisal, Tectonics 5 (1986) 797–8807.

[3] J.E.T. Channell, Palaeomagnetism and palaeogeography of Adria, in: A. Morris, D.H. Tarling (Eds.), Palaeomagnetism and Tectonics of the Mediterranean Region, Geol. Soc. Spec. Publ. 105 (1996) 119–132.

[4] R. Van der Voo, Paleomagnetism of the Atlantic, Tethys and Iapetus Oceans, Cambridge University Press, Cambridge, 1993, 411 pp.

[5] J.P. Platt, J.H. Behrmann, P.C. Cunningham, J.F. Dewey, M. Helman, M. Parish, M.G. Shepley, S. Wallis, P.J. Weston, Kinematics of the Alpine arc and the motion history of Adria, Nature 337 (1989) 158–161.

[6] G. Muttoni, M. Gaetani, K. Budurov, I. Zagorchev, E. Trifonova, D. Ivanova, L. Petrounova, W. Lowrie, Middle Triassic paleomagnetic data from northern Bulgaria: constraints on Tethyan magnetostratigraphy and paleogeography, Palaeogeogr. Palaeoclimatol. Palaeoecol. 160 (2000) 223–237.

[7] G. Muttoni, D.V. Kent, J.E.T. Channell, The evolution of Pangea: Paleomagnetic constraints from the Southern Alps, Italy, Earth Planet. Sci. Lett. 146 (1996) 107–120.

[8] D.V. Kent, P.E. Olsen, Implications of astronomical climate cycles to the chronology of the Triassic, Zbl. Geol. Paläont. 1 (Epicontinental Triassic International Symposium) (2000) 1463–1473.

[9] M.C. Chaouachi, A. M'Rabet, S. Razgallah, Les récifs du Permien supérieur du Jebel Tebaga de Medenine. Colloque Tuniso-Français de Sédimentologie, Livret Guide de l'Excursion Géologique, 1988.

[10] A. M'Rabet, S. Razgallah, M. Dridi, M.C. Chaouachi, Upper Permian reefs and associated siliciclastics at Jebel Tebaga, southern Tunisia, in: 17th Regional African–European Meeting of Sedimentology Field Trip Guide Book, Field Trip A1, International Association of Sedimentologists, 1996.

[11] G. Stampfli, J. Marcoux, A. Baud, Tethyan margins in space and time, Palaeogeogr. Palaeoclimatol. Palaeoecol. 87 (1991) 373–409.

[12] M. Gaetani, A. Arche, H. Kiersnowski, B. Chuvachov, S. Crasquin, M. Sandulescu, A. Seghedi, I. Zagorchev, A. Poisson, F. Hirsch, D. Vaslet, J. Le Metour, M. Ziegler, E. Abbate, L. Ait-Brahim, E. Barrier, S. Bouaziz, F. Bergerat, M.F. Brunet, J.P. Cadet, R. Stephenson, J.C. Guezou, A. Jabaloy, C. Lepvrier, G. Rimmele, Wordian paleogeographic map, in: J. Dercourt, M. Gaetani, B. Vrielynck, E. Barrier, B. Biju-Duval, M.-F. Brunet, J.-P. Cadet, S. Crasquin, M. Sandulescu (Eds.), Peri-Tethys Atlas and Explanatory Notes, Vol. 3, CCGM/CGMW, Paris, 2000, pp. 19–25.

[13] G. Cassinis, M. Avanzini, L. Cortesogno, G. Dellagiovanna, P. Di Stefano, L. Gaggero, M. Gullo, F. Massari, C. Neri, A. Ronchi, S. Seno, M. Vanossi, C. Venturini, Synthetic Upper Palaeozoic correlation charts of selected Italian areas, Atti Ticin. Sci. Terra 40 (1998) 65–120.

[14] F. Kilani-Mazraoui, S. Razgallah-Gargouri, B. Mannai-Tayech, The Permo-Triassic of Southern Tunisia – Biostratigraphy and palaeoenvironment, Rev. Palaeobot. Palynol. 66 (1990) 273–291.

[15] J.J. Mennig, P. Vittimberga, P. Lehmann, Etude sédimentologique et pétrographique de la Formation Ras Hamia (Trias moyen) du nord-ouest de la Lybie, Rev. Inst. Fr. Pet. 18 (1963) 1504–1519.

[16] A.N. Fatmi, B.A. Eliagoubi, O.S. Hammuda, Stratigraphic nomenclature of the pre-Upper Cretaceous Mesozoic rocks of Jabal Nafusah, NW Lybia, in: M.J. Salem, M.T. Busrewil (Eds.), The Geology of Libya, Vol. 2, Symposium on the Geology of Libya, 1980, pp. 57–65.

[17] A. Desio, C. Rossi Ronchetti, R. Pozzi, F. Clerici, G. Invernizzi, C. Pisoni, P.L. Viganò, Stratigraphic studies in the Tripolitanian Jebel (Libya), Riv. Ital. Paleontol. Stratigr. Mem. IX, 1963, 126 pp.

[18] R. Assereto, F. Benelli, Sedimentology of the pre-Cenomanian formations of the Jebel Gharian, Libya, in: C. Gray (Ed.), Symposium on the Geology of Libya, Faculty of Science, University of Libya, Tripoli, 1971, pp. 37–85.

[19] J.G.L.A. Van der Eem, Aspects of Midle and Late Triassic palynology. 6. Palynological investigations in the Ladinian and lower Carnian of the western Dolomites, Italy, Rev. Palaeobot. Palynol. 39 (1983) 189–300.

[20] C. Broglio Loriga, S. Cirilli, V. De Zanche, D. di Bari, P. Gianolla, G.F. Laghi, W. Lowrie, S. Manfrin, A. Mastandrea, P. Mietto, G. Muttoni, C. Neri, P. Posenato, M. Rechichi, R. Rettori, G. Roghi, The Prati di Stuores/Stuores Wiesen section (Dolomites, Italy): a candidate global stratotype section and point for the base of the Carnian stage, Riv. Ital. Stratigr. 105 (1999) 37–78.

[21] D.L. Martin, H.D. Munroe, A.E.M. Nairn, First results of the palaeomagnetic study of Libyan Mesozoic limestones: The Carnian Al Azizia Limestone Formation – preliminary data, in: M.J. Salem, A.M. Sbeta, M.R. Bakbak (Eds.), The Geology of Libya. Vol. VI, Elsevier, Amsterdam, 1991, pp. 2433–2440.

[22] W. Lowrie, Identification of ferromagnetic minerals in a rock by coercivity and unblocking temperature properties, Geophys. Res. Lett. 17 (1990) 159–162.

[23] J.L. Kirschvink, The least-squares line and plane and the analysis of palaeomagnetic data, Geophys. J. R. Astron. Soc. 62 (1980) 699–718.
[24] J.D.A. Zijderveld, A.C. demagnetization of rocks – analysis of results, in: D.W. Collinson, K.M. Creer, S.K. Runcorn (Eds.), Methods in Paleomagnetism, Elsevier, New York, 1967, pp. 254–286.
[25] M.W. McElhinny, Statistical significance of the fold test in palaeomagnetism, Geophys. J. R. Astron. Soc. 8 (1964) 338–340.
[26] P. Brack, G. Muttoni, High-resolution magnetostratigraphic and lithostratigraphic correlations in Middle Triassic pelagic carbonates from the Dolomites (northern Italy), Palaeogeogr. Palaeoclimatol. Palaeoecol. 161 (2000) 361–380.
[27] M.C. Van Fossen, D.V. Kent, A palaeomagnetic study of 143 Ma kimberlite dikes in central New York State, Geophys. J. Int. 113 (1993) 175–185.
[28] R.B. Hargraves, Paleomagnetism of Mesozoic kimberlites in Southern Africa and the Cretaceous apparent polar wander curve for Africa, J. Geophys. Res. 94 (B2) (1989) 1851–1866.
[29] M.B. Cita, F. Benelli, B. Bigioggeno, H. Chezar, A. Colombo, N.F. Sestini, L.R. Freeman, S. Iaccarino, F. Jadoul, E. Legnani, A. Malinverno, P. Massiotta, L. Paggi, I.P. Silva, Contribution to the geological exploration of the Malta Escarpment (eastern Mediterranean), Riv. Ital. Paleontol. Stratigr. 86 (1980) 317–355.
[30] R. Catalano, P. Di Stefano, H. Kozur, Permian circumpacific deep-water faunas from the western Tethys (Sicily, Italy) – New evidences for the position of the Permian Tethys, Palaeogeogr. Palaeoclimatol. Palaeoecol. 87 (1991) 75–108.
[31] R. Catalano, C. Doglioni, S. Merlini, On the Mesozoic Ionian Basin, Geophys. J. Int. 144 (2001) 49–64.
[32] E. Patacca, P. Scandone, M. Bellatalla, N. Perilli, U. Santini, The Numidian-sand event in the Southern Apennines, Mem. Sci. Geol. Padova 43 (1992) 297–337.
[33] L. Tauxe, P. Tucker, N.P. Petersen, J.L. Labrecque, The magnetostratigraphy of Leg 173 sediments, Palaeogeogr. Palaeoclimatol. Palaeoecol. 42 (1983) 65–90.
[34] D.A. Schneider, D.V. Kent, Paleomagnetism of Leg 115 sediments: Implications for Neogene magnetostratigraphy and paleolatitude of the Reunion hotspot, Proc. ODP Sci. Results 115 (1990) 717–736.
[35] J. Besse, V. Courtillot, Revised and synthetic apparent polar wander paths of the African, Eurasian, North American and Indian plates, and true polar wander since 200 Ma, J. Geophys. Res. 96 (B3) (1991) 4029–4050.
[36] J.P. Peixoto, A.H. Oort, The atmospheric branch of the hydrological cycle and climate, in: A. Street (Ed.), Variations of the Global Water Budget, Reidel, Dordrecht, 1983, pp. 5–65.
[37] D.V. Kent, P.E. Olsen, Magnetic polarity stratigraphy and paleolatitude of the Triassic–Jurassic Blomidon Formation in the Fundy Basin (Canada): Implications for early Mesozoic tropical climate gradients, Earth Planet. Sci. Lett. 179 (2000) 311–324.
[38] W.A. Brugman, H. Visscher, Permian and Triassic palynostratigraphy of northeast Libya, in: A. El-Arnauti, B. Owens, B. Thusu (Eds.), Subsurface Palynostratigraphy of Northeast Libya, Spec. Publ. Garyounis Univ., Benghazi 1988, 157–170.
[39] H. Visscher, C.J. Van der Zwan, Palynology of the Circum-Mediterranean Triassic: Phytogeographical and palaeoclimatological implications, Geol. Rundsch. 70 (1981) 625–634.
[40] M. Soussi, Ch. Abbes, H. Belayouni, N. Boukadi, Sédimentologie, stratigraphie séquentielle et caractéristiques géochimiques du Trias moyen et supérieur de l'Axe nord-sud (Tunisie centrale), Proceedings of the Fifth Tunisian Petroleum Exploration Conference, ETAP Mem. 10 (1996) 257–271.
[41] M. Soussi, S. Cirilli, Ch. Abbes, Palynological new data and precision on the age of the Triassic Rheouis Formation (Central Tunisia), Peri-Tethys Programme, ONAREP, Annual Meeting, 10–12 June, Rabat, 1997, pp. 84–85.
[42] R.L. Larson, E. Erba, Onset of the mid-Cretaceous greenhouse in the Barremian–Aptian Igneous events and the biological, sedimentary, and geochemical responses, Paleoceanography 14 (1999) 663–678.
[43] J.C. Van Wagoner, H.W. Posamentier, R.M. Mitchum, P.R. Vail, J.F. Sarg, T.S. Loutit, J. Hardenbol, An overview of the fundamentals of sequence stratigraphy and key definitions, S.E.P.M. Spec. Publ. 42 (1988) 39–45.
[44] G. Muttoni, D.V. Kent, P. Brack, A. Nicora, M. Balini, Middle Triassic magneto-biostratigraphy from the Dolomites and Greece, Earth Planet. Sci. Lett. 146 (1997) 107–120.
[45] M. Manzoni, Paleomagnetic data of Middle and Upper Triassic age from the Dolomites (eastern Alps, Italy), Tectonophysics 10 (1970) 411–424.
[46] J.D.A. Zijderveld, K.A. De Jong, Paleomagnetism of some Late Paleozoic and Triassic rocks from the eastern Lombardic Alps, Geol. Mijnbouw 48 (1969) 559–564.
[47] E. Marton, G. Nardi, Cretaceous palaeomagnetic results from Murge (Apulia, southern Italy); tectonic implications, Geophys. J. Int. 119 (1994) 842–856.